

## SWS observations of IR emission features towards compact HII regions<sup>\*</sup>

P.R. Roelfsema<sup>1,4</sup>, P. Cox<sup>2</sup>, A.G.G.M. Tielens<sup>3</sup>, L.J. Allamandola<sup>3</sup>, J.-P. Baluteau<sup>5</sup>, M.J. Barlow<sup>6</sup>, D. Beintema<sup>1,4</sup>, D.R. Boxhoorn<sup>1,4</sup>, J.P. Cassinelli<sup>7</sup>, E. Caux<sup>8</sup>, E. Churchwell<sup>7</sup>, P.E. Clegg<sup>9</sup>, Th. de Graauw<sup>1</sup>, A.M. Heras<sup>4</sup>, R. Huygen<sup>10</sup>, K.A. van der Hucht<sup>11</sup>, D.M. Hudgins<sup>3</sup>, M.F. Kessler<sup>4</sup>, T. Lim<sup>4,9</sup>, and S.A. Sandford<sup>3</sup>

<sup>1</sup> SRON, P.O. Box 800, 9700 AV Groningen, The Netherlands

<sup>2</sup> Institut d'Astrophysique Spatiale, Bât. 120, Université de Paris XI, F-91405 Orsay, France

<sup>3</sup> NASA Ames Research Center, MS: 245-6, Moffett Field, CA 94035, USA

<sup>4</sup> ISO Science Operations Centre, Astrophysics Division of ESA, P.O. Box 50727, E-28080 Madrid/Villafranca, Spain

<sup>5</sup> Laboratoire d'Astronomie Spatiale, CNRS, BP 8, F-13376 Marseille Cedex 12, France

<sup>6</sup> Department of Physics and Astronomy, University College London, Gower Street, London WC1E 6BT, UK

<sup>7</sup> Department of Astronomy, University of Wisconsin-Madison 475 N Charter Street, Madison, WI 53706-1582, USA

<sup>8</sup> Centre d'Etude Spatiale des Rayonnements, CESR/CNRS-UPS, BP 4346, F-31029 Toulouse Cedex, France

<sup>9</sup> Queen Mary and Westfield College, University of London, Mile End Road, London E1 4NS, UK

<sup>10</sup> Instituut voor Sterrenkunde, Universiteit van Leuven, Celestijnenlaan 200B, B-3001 Heverlee, Belgium

<sup>11</sup> SRON, Sorbonnelaan 2, 3584 CA Utrecht, The Netherlands

Received 31 July 1996 / Accepted 29 August 1996

**Abstract.** We present ISO Short Wavelength Spectrometer (SWS<sup>\*\*</sup>) grating spectra of six compact HII regions. In addition to strong emission lines from atomic species these spectra display infrared bands attributed to Polycyclic Aromatic Hydrocarbons (PAHs). The continuous spectral coverage of the present observations and the high spectral resolution allow to describe the detailed structure of the emission bands: the 7.7  $\mu\text{m}$  band is composed of two bands at 7.6 and 7.8  $\mu\text{m}$ , the 6.2  $\mu\text{m}$  band has a long wavelength extension, there is a plateau of emission between 6 and 7  $\mu\text{m}$  and a new feature is reported at 11.0  $\mu\text{m}$  in addition to the well-known 11.2  $\mu\text{m}$  band. These observations also reveal large variations in the relative intensities of the dust bands, in particular between the 7.7 and 8.6  $\mu\text{m}$  bands. In one extreme case, the 8.6  $\mu\text{m}$  band is stronger than the 7.7  $\mu\text{m}$  band. These observations are compared to a mixed population of ionized PAHs, using new laboratory measurements.

**Key words:** ISM: dust – ISM: HII regions – ISM: molecules – infrared: ISM: lines and bands

<sup>\*</sup> Based on observations with ISO, an ESA project with instruments funded by ESA Member States (especially the PI countries: France Germany, the Netherlands and the United Kingdom) and with the participation of ISAS and NASA.

<sup>\*\*</sup> SWS is a joint project of SRON and MPE (DARA grants no 50 QI9402 3 and 50 QI8610 8) with contributions from KU Leuven, Steward Observatory, and Phillips Laboratory.

### 1. Introduction

A series of prominent near- and mid-infrared emission bands seen in a variety of sources including reflection nebulae, HII regions, planetary nebulae, the diffuse interstellar medium and galaxies are generally attributed to a family of aromatic hydrocarbon species (Puget & Léger 1989; Allamandola et al. 1989 and references therein). The exact nature of these small particles has been a matter of considerable debate over the last decade: the most widely accepted identification is that of PAHs (Léger & Puget 1984; Allamandola et al. 1985) either neutral or ionized. While other carriers have been proposed including hydrogenated amorphous carbons (HACs; Borghesi et al. 1987), quenched carbonaceous compounds (QCCs; Sakata et al. 1984) and coal grains (Papoular et al. 1989), none is able to explain the excitation process satisfactorily.

The SWS on board the Infrared Space Observatory (ISO, see Kessler et al. 1996) with its large coverage in wavelength and spectral resolution provides a unique opportunity to probe in detail the dust spectral signatures in a vast number of sources spanning a wide range of physical conditions. Such a data base will enable, amongst other work, to study how the carriers of the broad dust emission bands vary from source to source and explore the reasons for these changes.

This Letter presents the results of an on-going ISO spectroscopic guaranteed time program devoted to the study of compact HII regions in the Galaxy. Here, we concentrate on the infrared

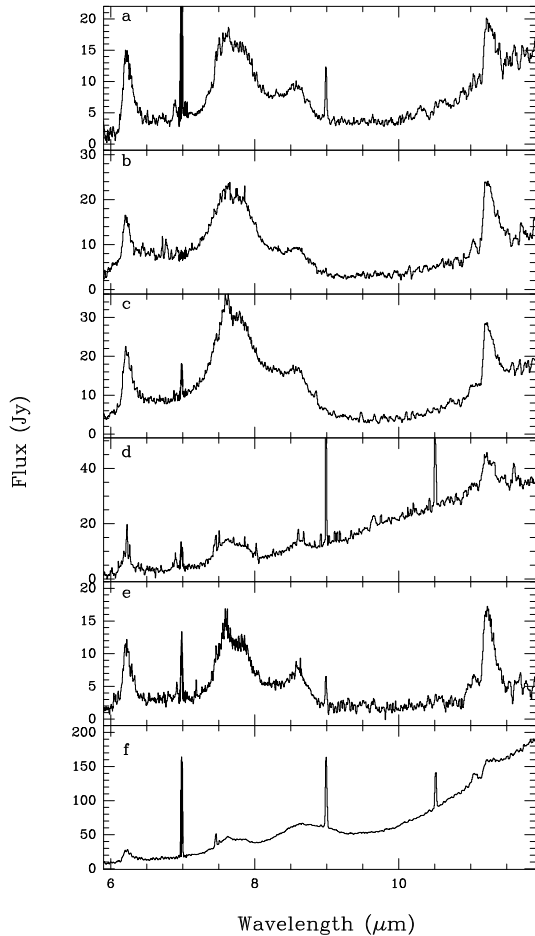


**Fig. 1.** The ISO SWS spectra of six compact HII regions between 6 and 12  $\mu\text{m}$ . The sources are IRAS: 18116–1646 (a), 18162–2048 (b), 19442+2427 (c), 21190+5140 (d), 22308+5812 (e) and 18434–0242 (f)

emission features in six compact HII regions. A description of the SWS is given by de Graauw et al. (1996), and the wavelength and flux calibration are described in Valentijn et al. (1996) and Schaeidt et al. (1996), respectively.

## 2. Observations and results

We selected six representative cases of compact HII regions from the sources observed to date (Table 1). The observations were carried out using the SWS AOT01 full scan observing mode, at speed 2. The spectra were reduced using the standard SWS Interactive Analysis (IA) reduction programs. The absolute flux calibration was based on calibration files available in version 4.1 of the off-line processing pipeline. In this paper we concentrate on the region between 6 and 12  $\mu\text{m}$  corresponding to bands 1 and 2 of the SWS where the calibration accuracy is estimated to be of the order of 20%. The spectra are displayed in Fig. 1 rebinned to a resolution of 400. Fig. 2 shows the same data continuum subtracted. In Table 1 the distance to the sun ( $D_{\text{sun}}$ ), and total luminosity ( $L_{\text{tot}}$ ) are listed together with the intensity ratios for the observed dust emission bands.

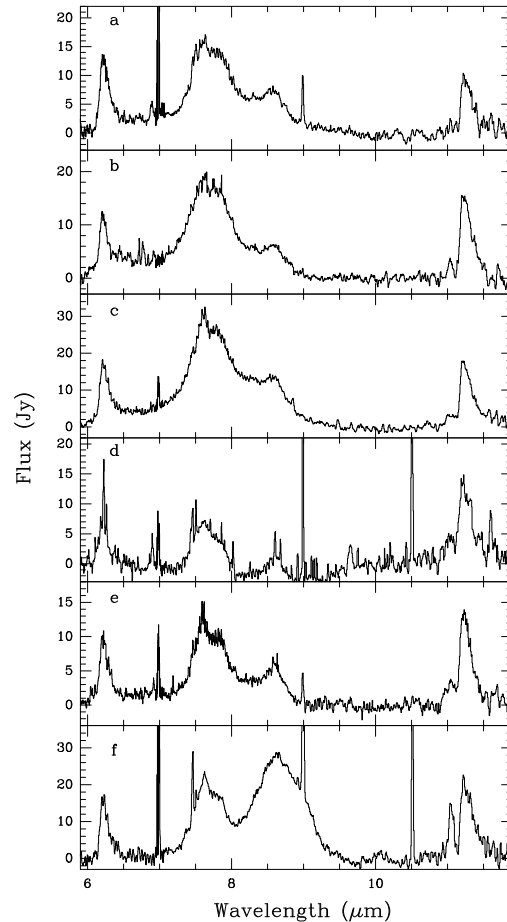


**Fig. 2.** Continuum subtracted SWS 6–12  $\mu\text{m}$  spectra of the six compact HII regions shown in Fig. 1

The six compact HII regions show a very rich spectrum between 6 and 12  $\mu\text{m}$  with intense atomic fine-structure lines of [ArII], [ArIII], [SIV] and  $\text{Pf}\alpha$  (a detailed discussion of the atomic lines will be given in a forthcoming paper), and the series of broad and strong emission bands at 6.2, 7.7, 8.6 and 11.2  $\mu\text{m}$ . The quality of the present data allows one to distinguish many more details than in previous studies (e.g., Cohen et al. 1989) as well as to detect new weak dust bands.

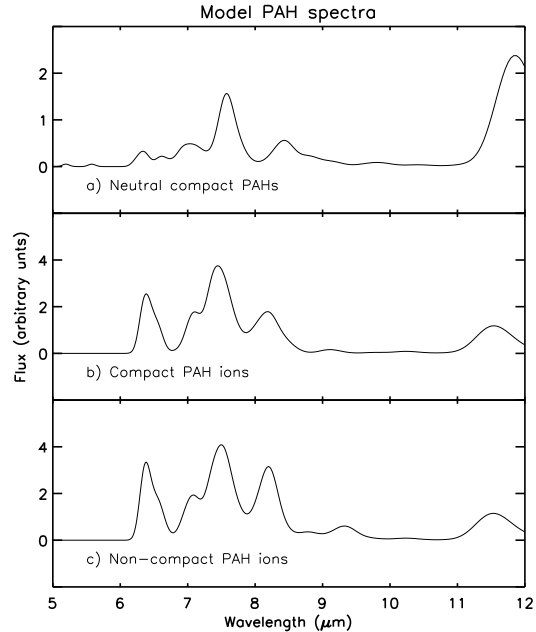
The 6.2  $\mu\text{m}$  dust band extends from 6.08 to 6.5  $\mu\text{m}$  with a steep increase on the short wavelength side and a pronounced wing at longer wavelengths. The apparent excess emission plateau between 6.4 and 7.2  $\mu\text{m}$  is likely to be related to C–C stretching modes of carbon-related particles and could be due to a series of unresolved emission bands (Allamandola et al. 1985). The 7.7  $\mu\text{m}$  band extends from 7.2 to 8.1  $\mu\text{m}$  and appears to be composed of two emission bands: the strongest one peaking at 7.60  $\mu\text{m}$  and the second weaker one at 7.85  $\mu\text{m}$ . This double peak is also seen in other types of sources (Bregman 1989, Beintema et al. 1996, Molster et al. 1996). The 8.6  $\mu\text{m}$  band extends to  $\sim 8.90$   $\mu\text{m}$  and until the next band at 11  $\mu\text{m}$  the continuum level is very low coming back to the level it had just before the start of the 6.2  $\mu\text{m}$  band. This reinforces the impression that, in most cases, the 6.1 to 8.9  $\mu\text{m}$  region mainly

**Table 1.** Properties of the sources and relative intensities. The values on the bottom line are from Cohen et al. (1989).

IRAS name	$D_{\text{sun}}$ (kpc)	$L_{\text{tot}}$ ( $10^4 L_{\odot}$ )	Intensity ratio				
			3.3 11.2	6.2 7.6	7.6 8.6	7.6 11.2	11.04 11.20
18116–1646	4.4	15.8	0.25	0.50	5	11	$\leq 0.2$
18162–2048	1.9	2.8	0.15	0.10	5	11	0.1
19442.2427	2.3	5.4	0.25	0.25	6	11	$\leq 0.2$
21190.5140	6.8	13.5	0.25	0.30	7	5	0.2
22308.5812	5.7	8.8	0.30	0.30	9	8	0.2
18434–0242	7.4	22.2	0.35	0.20	0.6	6	0.3
typical HII region:			0.43	0.58	-	3	-

consists of emission bands with little or no continuum emission (exceptions are IRAS 21190+5140 and IRAS 18434-0242 where the mid-infrared continuum is very strong - Fig. 1d and f). This high feature to continuum ratio strengthens the idea that these infrared emission features are carried by molecular-sized species which emit in well-defined bands rather than dust grains which would emit in continuum as well. The well-known 11  $\mu\text{m}$  band peaks at 11.20  $\mu\text{m}$  and also displays an asymmetric shape towards longer wavelengths (Witteborn et al. 1989). Besides the 11.20  $\mu\text{m}$  feature, an additional feature at 11.04  $\mu\text{m}$  is present which, in most cases, is much weaker than the 11.20  $\mu\text{m}$  band. In the case of IRAS 18434-0242, the 11.04  $\mu\text{m}$  band is very strong with an intensity almost half that of the 11.20  $\mu\text{m}$  band (Fig. 2f). Such a secondary 11.04  $\mu\text{m}$  emission feature has been reported earlier by Roche et al. (1991).

The relative intensities of the PAH bands in the wavelength region from 6 to 12  $\mu\text{m}$  display significant variations from source to source (Table 1). Note that the emission band at 3.3  $\mu\text{m}$  (not shown in this paper - a full discussion of the complete set of dust bands in the infrared regime is deferred to a subsequent paper) is also included for completeness. The most dramatic change in relative intensities is seen between the 7.6 and 8.6  $\mu\text{m}$  bands. In most of the sources observed to date, the 7.6  $\mu\text{m}$  band is stronger than the 8.6  $\mu\text{m}$  band by a factor 5-10. However, in the case of IRAS 18434-0242, the 8.6  $\mu\text{m}$  band is almost twice as strong as the 7.6  $\mu\text{m}$  band. Similar trends are also reported by Joblin et al. (1996) for the 8.6/11.2  $\mu\text{m}$  ratio in the reflection nebula NGC 1333 and by Verstraete et al. (1996) towards the HII region of M 17. A change in relative intensities is also seen between the 11.04 and 11.20  $\mu\text{m}$  bands. The 11.04  $\mu\text{m}$  band is typically up to 1/5 of the 11.20  $\mu\text{m}$  band except in IRAS 18434-0242 where the ratio has a value of 0.3. The strength of the 11.04  $\mu\text{m}$  feature could be related to that of the 8.6  $\mu\text{m}$  bands. Finally, the relative intensities of 3.3 to 11.2  $\mu\text{m}$  and 6.2 to 7.6  $\mu\text{m}$  do not appear to show large variations from source to source (apart from IRAS 18162-2048). The typical ratios for these bands are found to be 0.25 and 0.3, respectively, somewhat below the average values found by Cohen et al. (1989).

**Fig. 3.** Laboratory measurements between 5 and 12  $\mu\text{m}$  of neutral compact PAHs, compact PAH ions, non-compact PAH ions (from top to bottom). See text for details

### 3. Discussion

Likely, the infrared emission features are not due to a single carrier but instead represent emission from a whole family of species. Moreover, these PAHs are probably ionized by the strong UV radiation field in the photon-dissociation regions surrounding the HII regions. In order to further identify this family of carriers and to study the relative intensities of the mid-infrared bands reported above, the spectra of a number of neutral and ionized PAHs, isolated in Argon matrices, were measured at the Astrochemistry Laboratory at NASA Ames (Hudgins et al. 1994; Hudgins & Allamandola 1995). The width of the absorption features measured in the laboratory is dominated by solid state effects, i.e. interaction with the matrix. In contrast, the linewidth of IR emission features from vibrationally hot molecules is dominated by non-radiative energy redistribution among many levels (Jortner et al. 1969). The observed linewidth of the narrowest interstellar emission bands ( $\approx 50 \text{ cm}^{-1}$ ) is consistent with measured rates for intramolecular energy transfer between the vibrational modes. Hence for each PAH, using measured peak positions and relative strength of the various IR absorption bands, an intrinsic emission spectrum has been constructed adopting a gaussian line profile with a FWHM of  $50 \text{ cm}^{-1}$ . These theoretical emission spectra have then been summed over a distribution of PAHs in various ionization stages. No correction for the emission temperature ( $\approx 500 \text{ K}$ ) has been applied, since over the relevant wavelength range such corrections would be small.

The spectrum of a collection of neutral PAHs is shown in Fig 3a. We concentrate here on compact PAHs, which are thermodynamically most stable. As is well known, the spectra of neutral PAHs are dominated by the out-of-plane C-H bending

modes longwards of 11  $\mu\text{m}$  which are much stronger than the C-C modes near 6.2 and 7.7  $\mu\text{m}$  and C-H in-plane bending mode near 8.6  $\mu\text{m}$  (Fig. 3a). Upon ionization of this same set of compact PAHs, the C-C stretching modes and C-H in-plane bending modes grow in intrinsic intensity relative to the C-H out-of-plane bending modes (Allamandola et al. 1995; Vala et al. 1994; Hudgins and Allamandola 1995; Langhoff 1996). The resulting spectrum resembles the generally observed emission spectrum fairly well both in peak position and relative intensity (Fig. 2a-c). We note in passing that, due to blending, the asymmetry of the 6.2  $\mu\text{m}$  feature is well reproduced. Inspired by a cursory inspection of Fig. 2, we have searched our data base of PAH spectra to select a sample which enhances the contribution in the vicinity of the 8.6  $\mu\text{m}$  emission feature. The results are shown in Fig. 3c. While the PAH mixture still contains a fair number of condensed PAH structures, the addition of less condensed PAHs specifically enhances the 8.6  $\mu\text{m}$  region.

As this study demonstrates, the spectral appearance of the interstellar PAH spectrum is very sensitive to changes in the PAH population. Conversely, observed variations can thus be used to probe the detailed composition of interstellar PAHs. The general IR emission spectra is well matched by a collection of small, compact PAHs. We interpret the observed variations - the strong 8.6  $\mu\text{m}$  band, the appearance of an 11.0  $\mu\text{m}$  band and the increased 7.8  $\mu\text{m}$  shoulder - as evidence for the presence of less stable non-compact PAHs in some sources. In support of this hypothesis, we note that those sources which show these features to be the strongest tend to have higher total luminosities (Table 1). In sources with high excitation conditions, such as IRAS 18434-0242, the population of interstellar PAHs is subjected to intense and rapid FUV processing. Likely, this erosion process leads to the formation of non-compact PAHs. In contrast, in the other sources, the PAH population resembles more directly that of the general ISM where formation and destruction processes, operating over  $10^9$  yrs, have lead to a steady state distribution which concentrates on the more stable compact PAHs.

#### 4. Conclusions

The population of interstellar PAHs is expected to be very wide and diverse. As a result, the PAH population of any specific source will be very sensitive to the local physical conditions. The spectra of compact HII regions presented here show a first hint of this spectral diversity. The SWS on ISO will make available a large set of homogenous spectra on a variety of sources. Such a data set, in combination with a dedicated laboratory study of a wide variety of PAHs, will enable us to disentangle the contribution from the individual PAHs and ultimately to reach the holy grail: the identification of the grandPAHs of them all.

*Acknowledgements.* We are greatly indebted to the SWS Instrument Dedicated Team (SIDT) at VILSPA for their support in the calibration and analysis of SWS data.

#### References

- Allamandola, L.J., Tielens, A.G.G.M., Barker, J.R. 1985, ApJ, 290, L25  
 Allamandola, L.J., Tielens, A.G.G.M., Barker, J.R. 1989, ApJ Supp, 71, 733  
 Allamandola, L.J., Sandford, S.A., Hudgins, D.M., Witteborn, F.C., 1995, ASP Conf 73, 23  
 Beintema, D.A., van den Ancker, M.E., Molster, F.J. et al. 1996, this issue  
 Borghesi, A., Bussoletti, E., Colangeli, L. 1987, ApJ, 314, 422  
 Bregman, J.: 1989, in *Interstellar Dust*, IAU Symp. 135, eds. L.J. Allamandola, A.G.G.M. Tielens, p. 109  
 Cohen, M., Tielens, A.G.G.M., Bregman, J. et al. 1989, ApJ, 341, 246  
 de Graauw, Th., Haser, L.N., Beintema, D.A. et al. 1996, this issue  
 Hudgins, D.M., Sandford, S.A., Allamandola, L.J. 1994, J. Ph. Chem., 98, 4243  
 Hudgins, D.M., Allamandola, L.J. 1995, J. Ph. Chem., 99, 3033  
 Joblin, C., Tielens, A.G.G.M., Geballe, T., Wooden, D.H. 1996, ApJ, 460, L119  
 Jortner, J., Rice, S.A., Hochstrassen, R.M. 1969, Adv. Photochemistry, 7, 148  
 Kessler, M.F. et al. 1996, this issue  
 Langhoff, S.R. 1996, J. Ph. Chem. 100, 2819  
 Léger, A., Puget, J.-L. 1984, AA, 137, L5  
 Molster, F.J., van den Ancker, M.e., Tielens, A.G.G.M. et al. 1996, this issue  
 Papoular, R., Conrad, J., Giuliano, M. et al. 1989, AA, 217, 204  
 Puget, J.-L., Léger, A. 1989, AARA, 67, 161  
 Roche, P.F., Aitken, D.K., Smith, C. 1991, MNRAS, 252, 282  
 Sakata, A., Wada, S., Tanabe, T., et al. 1984, ApJ, 287, L51  
 Schaeidt, S.G., Morris, P.W., Salama, A. et al. 1996, this issue  
 Vala, M., Szczepanski, J. Puzat, F. et al. 1994, J. Ph. Chem., 98, 9187  
 Valentijn, E.A., Feuchtgruber, H., Kester, D.J.M. et al. 1996, this issue  
 Verstraete, L. et al. 1996, this issue  
 Witteborn, F.C., Sandford, S.A., Breaman, T.D., et al. 1989, ApJ, 341, 270